EFDA–JET–CP(14)06/40

C.D. Challis, J. Garcia, M. Beurskens, P. Buratti, P. Drewelow, L. Frassinetti, C. Giroud, N. Hawkes, J. Hobirk, E. Joffrin, D. Keeling, D.B. King, C. Marchetto, J. Mailloux, D. McDonald, I. Nunes, G. Pucella, S. Saarelma, J. Simpson and JET EFDA contributors

Improved Confinement in JET High β Plasmas with an ITER-Like Wall

Improved Confinement in JET High β Plasmas with an ITER-Like Wall

C.D. Challis[1], J. Garcia[2], M. Beurskens[1], P. Buratti[3], P. Drewelow[4], L. Frassinetti[5], C. Giroud[1], N. Hawkes[1], J. Hobirk[4], E. Joffrin[2], D. Keeling[1], D.B. King[1], C. Marchetto[6], J. Mailloux[1], D. McDonald[7], I. Nunes[8], G. Pucella[3], S. Saarelma[1], J. Simpson[1] and JET EFDA contributors*

JET-EFDA, Culham Science Centre, OX14 3DB, Abingdon, UK

[1]*EURATOM-CCFE Fusion Association, Culham Science Centre, OX14 3DB, Abingdon, OXON, UK*
[2]*CEA, IRFM, F-13108 Saint-Paul-lez-Durance, France*
[3]*Unità Tecnica Fusione, C.R. ENEA Frascati, CP65, 00044 Frascati, Italy*
[4]*Max-Planck-Institut für Plasmaphysik, D-85748 Garching, Germany*
[5]*VR, Fusion Plasma Physics, KTH, SE-10044 Stockholm, Sweden*
[6]*Instituto di Fisica del Plasma, CNR, 20125 Milano, Italy*
[7]*EFDA CSU Garching, D-85748 Garching, Germany*
[8]*Instituto de Plasmas e Fusão Nuclear, IST, Universidade de Lisboa, Portugal*
** See annex of F. Romanelli et al, "Overview of JET Results", (25th IAEA Fusion Energy Conference, Saint Petersburg, Russia (2014)).*

Preprint of Paper to be submitted for publication in Proceedings of the 25th IAEA Fusion Energy Conference, St Petersburg, Russia 13th October 2014 - 18th October 2014

ABSTRACT.
The replacement of the JET carbon wall (C-wall) by a Be/W ITER-like wall (ILW) has affected the plasma energy confinement. To investigate this, experiments have been performed with both the C-wall and ILW to vary the heating power over a wide range for plasmas with different shapes. It was found that the power degradation of thermal energy confinement was weak with the ILW; much weaker than the IPB98(y,2) scaling and resulting in an increase in normalised confinement from $H_{98} \sim 0.9$ at $\beta_N \sim 1.5$ to $H_{98} \sim 1.2$–1.3 at $\beta_N \sim 2.5$–3.0 as the power was increased (where $H_{98} = \tau_E/\tau_{IPB98(y,2)}$ and $\beta_N = \beta_T B_T/aI_P$ in %·T/m·MA). This reproduces the general trend in JET of higher normalised confinement in the so-called 'hybrid' domain, where β_N is typically above 2.5, compared with 'baseline' ELMy H-mode plasmas with $\beta_N \sim 1.5$–2.0. This weak power degradation of confinement, which was also seen with the C-wall experiments at low triangularity, is associated with both increased edge pedestal pressure and core pressure peaking at high power. By contrast, the high triangularity C-wall plasmas exhibited elevated H_{98} over a wide power range with strong, IPB98(y,2)-like, power degradation. This strong power degradation of confinement appears to have been linked to an increase in the source of neutral particles from the wall as the power increased; an effect that was not reproduced with the ILW. The reason for the loss of improved confinement domain at low power with the ILW is yet to be clarified, but contributing factors may include changes in the rate of gas injection, wall recycling, plasma composition and radiation. The results presented in this paper show that the choice of wall materials can strongly affect plasma performance, even changing confinement scalings that are relied upon for extrapolation to future devices.

1. INTRODUCTION

The replacement of the JET carbon wall by an ITER-like wall, composed of beryllium for the main chamber wall and tungsten in the divertor, has affected plasma energy confinement in two ways: (i) by the effect of the wall materials on key plasma parameters, e.g. through plasma composition and wall recycling; and (ii) by operational techniques necessary to avoid damage to plasma facing components (PFCs) and maintain stable plasma conditions, e.g. gas injection to avoid tungsten accumulation. This has generally resulted in a reduction in confinement for ELMy H-mode plasmas in the ITER baseline domain ($\beta_N < 2$) compared with previous C-wall experiments and the IPB98(y,2) confinement scaling [1,2]. By contrast, hybrid plasmas at high β_N exhibit similar confinement quality with the carbon and metal PFCs, significantly exceeding the IPB98(y,2) scaling in both cases [3].

These observations have motivated an investigation of the energy confinement scaling with applied heating power with the ILW to compare with previous experiments performed with the C-wall. It is well known that plasma confinement is sensitive to the plasma shape (e.g. [4]) and analysis of the JET C-wall experiments has shown that changes in plasma shape can also modify the scaling of energy confinement with power [5]. It is believed that this effect was largely due to the source of neutral particles resulting from plasma-wall interactions in the main chamber. Consequently the ILW experiments were performed using two different plasma shapes to investigate the impact of

the change of wall materials on the shape dependence of confinement. This has resulted in a C-wall and ILW database comprising four power scans performed with two different plasma shapes and two different PFC arrangements.

2. OVERVIEW OF POWER SCAN EXPERIMENTS

The time evolution of typical plasmas from the C-wall and ILW power scan experiments are shown in Figure 1. The plasma current waveform shows a 'current overshoot' before the Neutral Beam Injection (NBI) pulse. This forms a wide region of low magnetic shear in the plasma interior with $q_0 \sim 1$, which provides access to the hybrid domain with high β_N and $H_{98} > 1$ [6]. Thus the experiments described in this paper are representative of JET hybrid plasmas at high power and, in terms of β_N, overlap with the baseline domain at low power.

The two plasma shapes, illustrated in Figure 2, have low and high triangularity (δ), respectively. The divertor geometry was different for the C-wall and ILW power scans and the effect of this on confinement has been studied with the ILW. The small change in geometry in the high δ scans did not result in a significant change in confinement. At low δ the divertor strike-points were much closer to the cryopump with the C-wall, which can give a higher energy confinement by ~ 10%. However, in the ILW studies this effect was consistent over a range of power levels such that the power scaling of confinement was not affected by the change in divertor geometry. A more thorough investigation of the effect of divertor geometry with the JET ILW is presented in [7].

A higher gas injection rate was used during the main heating phase in the ILW power scans compared with the C-wall experiments to avoid rapid plasma contamination by high Z impurities, which can cause radiation cooling and a collapse of the plasma stored energy. Although impurity accumulation can be mitigated by gas injection, the required gas flow rates can also degrade the plasma energy confinement [8]. Consequently, the gas injection rate for the ILW power scans was set as low as possible to provide good ELMy H-mode confinement for comparison with the C-wall plasmas while ensuring that any rise in plasma radiation was on a timescale much longer than the energy confinement time. As a result the conditions for the ILW power scans are not representative of fully stationary plasmas and the radiated power fraction varied in both magnitude and dependence on heating power in the four power scans. The implications of this for the energy confinement analysis are discussed in the next section.

Three of the four power scans were performed at the same plasma current and magnetic field (1.4MA/1.7T), the exception being the C-wall low δ plasmas, which were at 1.7MA/2.0T. All four power scans were performed at similar values of q_{95} (~ 3.9). In each power scan the start time of the NBI main heating pulse was kept constant, as was the time of the confinement analysis. This was chosen to be after the plasma stored energy had become roughly steady while being close enough to the start of the NBI heating pulse to avoid significant changes in the q-profile shape as the heating power was varied. The q-profile at the analysis time is illustrated for each of the power scans in Figure 3. The similarity of the q-profiles indicates that the current profiles obtained in the

C-wall plasmas were largely reproduced in the ILW experiments. The slightly higher value of q_0 for the low δ C-wall plasmas is consistent with the observation of electron temperature sawteeth just before the analysis time at low power in all cases except the low δ C-wall plasmas. Nevertheless, the observation of steady confinement conditions in low δ C-wall plasmas up to and including the sawtoothing phase suggests that such small differences in the q-profile shape are unlikely to have significant effect on the overall plasma energy confinement. The presence of sawteeth in some plasmas does, however, increase the risk of triggering tearing modes, and plasmas with confinement degrading modes (e.g. with n = 2) were excluded from the confinement analysis.

In conclusion, the C-wall and ILW power scans are comparable in terms of plasma shapes and q-profiles. The differences in divertor geometry appear to have introduced a ~10% variation in confinement in the low δ comparison, but there is no evidence that it has affected the power scaling of confinement. The necessity for a higher gas injection rate with the ILW may also have affected the confinement, but the gas flow rate was minimized to mitigate, as far as possible, the impact of this on the comparison. The resulting dataset allows a comparison of the confinement behaviour with the JET C-wall and ILW in conditions of minimal gas injection where the most significant differences are the wall materials themselves.

3. CONFINEMENT ANALYSIS

Each power scan was performed with the other key 'engineering' variables as constant as possible. The plasma current, magnetic field, major radius, aspect ratio and elongation were all maintained within ±1.3% for each individual power scan. The main ion species was deuterium with typically less than 3% hydrogen and the line average electron density variation was no more than ±5% within each power scan. Two pulses were omitted from the analysis dataset because they had higher density than was typical for the relevant power scan. The achievement of essentially constant conditions in terms of the key 'engineering' variables during each of the power scan experiments allows a direct measurement of the dependence of plasma energy confinement on heating power in the different wall environments.

The plasma profiles are illustrated at two power levels for the four power scans in Figure 4. The density was lower in the low δ plasmas, which is a typical observation for JET C-wall and ILW experiments. The density was lowest in the C-wall low δ experiments, which is consistent with the optimization of the divertor geometry for pumping in this scan. With the exception of the C-wall high δ plasmas the main effect of increasing the heating power was to increase the temperature across the whole plasma radius, especially for the ions. In the C-wall high δ plasmas the temperature rise was negligible in the plasma periphery, although some increase in temperature peaking is evident. This resulted in stronger power degradation of confinement for the high δ C-wall plasmas compared with the other three cases.

Figure 5 shows the plasma thermal stored energy, evaluated by integrating the measured plasma profiles, as a function of the absorbed heating power for each of the power scans. The stored energy

expected from the IPB98(y,2) scaling is also shown, and H_{98} can be estimated from the ratio of the measurements to the IPB98(y,2) curves. Both of the ILW power scans and the C-wall scan at low δ all exhibit a substantially faster increase in plasma stored energy than expected from the IPB98(y,2) scaling, leading to an increase in H_{98} above unity at high power. The exception is the C-wall high δ power scan, which has $H_{98}>1$ at all levels of power. In this case the thermal stored energy increases slowly as the power is increased, following a similar power dependence to the IPB98(y,2) scaling. Since β scales with plasma stored energy in each power scan the dependences shown in Figure 5 are consistent with the general observation in JET ILW experiments of higher H_{98} in hybrid plasmas at high β_N compared with baseline ELMy H-mode plasmas in the domain $\beta_N < 2$. The observation of strong power degradation only in the C-wall high δ plasmas suggests that some special factor is responsible for the power dependence in this case.

The change in wall material in JET has resulted in changes in the plasma impurity composition and, consequently, radiation losses. In Figure 6 the thermal stored energy is plotted as a function of the net loss power for the four power scans in this experiment. Here the net loss power is defined as the difference between the absorbed heating power and the power radiated from within the last closed flux surface. From these observations it is clear that neither the weak power degradation of confinement with the ILW nor the differences with respect to the high δ C-wall power scan can be explained by the changes in radiation behaviour from within the confined plasma due to the use of different wall materials.

The contribution of the H-mode pedestal to the overall energy confinement has been estimated for the plasmas in this experiment. The C-wall low δ power scan was excluded because high resolution Thomson scattering data was not available for the majority of the plasmas. The boundary between the pedestal and core regions was fixed at $\rho_{tor}= 0.89$, as illustrated in Figure 4 and the contribution of the pedestal pressure, W_{ped}, was evaluated by integrating the plasma profiles with the thermal pressure set to the boundary value in the region $\rho_{tor}< 0.89$. The ion temperature was assumed to be equal to the electron temperature in the pedestal region and the contribution of the plasma core was characterised by the core energy, $W_{core}= W_{th}–W_{ped}$.

Figure 7 shows that the pedestal energy increase with power is very weak for the C-wall power scan at high δ, suggesting that the pedestal behaviour is a key factor in strong power degradation of confinement in this case. This correlates with an observed increase in the Dα emission from the tokamak mid-plane line-of-sight, as seen in Figure 8. The Dα emission was roughly constant with power for the other power scans, but indicates a collinear increase in main chamber neutral particle population with power for the high δ C-wall plasmas. It is believed that this increase is responsible for the different power degradation of confinement in this case [5]. A more thorough analysis of this issue using additional diagnostics and an assessment of candidate physics explanations for the effect on confinement will be discussed in a separate publication. The core energy increases more rapidly with power than the pedestal energy for all three scans in Figure 7, indicating that the plasma core also contributes significantly to the observed confinement scaling.

The variations in temperature and density peaking with power are shown in Figure 9. Here the peaking factor is defined as the ratio of the volume average to the pedestal value so as to quantify the relative contribution of the core to the global integral. It can be seen that the contribution of temperature peaking to the increase in core pressure with heating power is comparable for the three power scans. In the case of the ILW experiments the ion temperature peaking increase is the dominant factor, while the high δ C-wall data shows similar peaking changes for both profiles, as seen in Figure 4. By contrast, the electron density peaking behaves differently for the three power scans. It is essentially constant with power in the C-wall high triangularity plasmas, increases gradually with power for high δ ILW plasmas and rises most rapidly with power in the low δ ILW scan.

The electron density peaking was highest in the low δ experiments and tended to increase with heating power in all cases except the C-wall high δ plasmas. This resulted in a correlation between density peaking and collisionality, as shown in Figure 10, consistent with previous observations in ASDEX Upgrade and JET [9]. It should be noted that the central fuelling due to NBI also increased with heating power in each of the scans and it was not possible to decouple the effects of collisionality and fuelling in these experiments. Nevertheless the contribution of electron density peaking to the rapid increase of plasma stored energy with heating power in three of the four power scans discussed in this paper is consistent with the previously observed behaviour in a wider database.

CONCLUSIONS

Dedicated power scans have been performed at JET to investigate the scaling of plasma energy confinement with different plasma shapes and first wall materials using minimal gas injection rates and spanning the range of β_N between 'baseline' ELMy H-mode plasmas (~ 1.5–2.0) and the 'hybrid' domain (~ 2.5–3.0). It has been concluded that the C-wall high triangularity power scan, which was the only case to exhibit strong power degradation of confinement, was atypical of the confinement behaviour in the JET tokamak. This exceptional case appears to have been affected by variations in the neutral particle population in the main chamber. All the other power scans showed weak power degradation of confinement, much weaker than the IPB98(y,2) scaling. This is consistent with previous observations of weak β scaling of confinement in ELMy H-mode plasmas in DIII-D and JET [10]. The observed rapid increase in plasma stored energy with power is due to an increase in both pedestal pressure and core pressure peaking. The pedestal pressure increase is generally consistent with peeling-ballooning paradigm, the density peaking increase is consistent with the previously observed correlation with collisionality and the temperature peaking increase suggests the relevance of transport factors such as the effect of suprathermal pressure [11].

It should be noted that the various factors responsible for the rapid rise in plasma stored energy with power are not independent. The increase in the core pressure results in an increase in global β, which can affect pedestal stability. Conversely, the increase in pedestal pressure can affect the core pressure if core transport processes are sensitive to gradient scale lengths. Thus the confinement scaling with power may be determined by a complex interplay between a variety of physics

mechanisms [12]. The sensitivity of these mechanisms to β may explain the observation of stronger power degradation of confinement at low β with the JET ILW [3]. The weak power degradation of confinement observed in these experiments is encouraging for the development of high gain fusion devices where heating power and plasma β are high.

ACKNOWLEDGEMENTS

This work was supported by EURATOM and carried out within the framework of the European Fusion Development Agreement. The views and opinions expressed herein do not necessarily reflect those of the European Commission. This work was also part-funded by the RCUK Energy Programme under grant EP/I501045.

REFERENCES

[1]. ITER Physics Basis 1999 Nuclear Fusion **39** 2175
[2]. Beurskens M.N.A et al., 2013 Plasma Physics and Controlled Fusion **55** 124043
[3]. Beurskens M.N.A. et al., 2014 Nuclear Fusion **54** 043001
[4]. Osborne T.H. et al., 2000 Plasma Physics and Controlled Fusion **42** A175
[5]. Joffrin E. et al., 2014 Proc 41st EPS Conf on Plasma Phys (Berlin, Germany, 2014) O4.125
[6]. Hobirk J. et al., 2013 Plasma Physics and Controlled Fusion **54** 095001
[7]. Joffrin E. et al., this conference EX/P3-40
[8]. Joffrin E. et al., 2014 Nuclear Fusion **54** 013011
[9]. Angioni C. et al., 2007 Nuclear Fusion **47** 1326
[10]. Luce T.C. et al., 2008 Plasma Physics and Controlled Fusion **50** 043001
[11]. Citrin J. et al., 2013 Physical Review Letters **111** 155001
[12]. Garcia J. et., al this conference TH/5-2

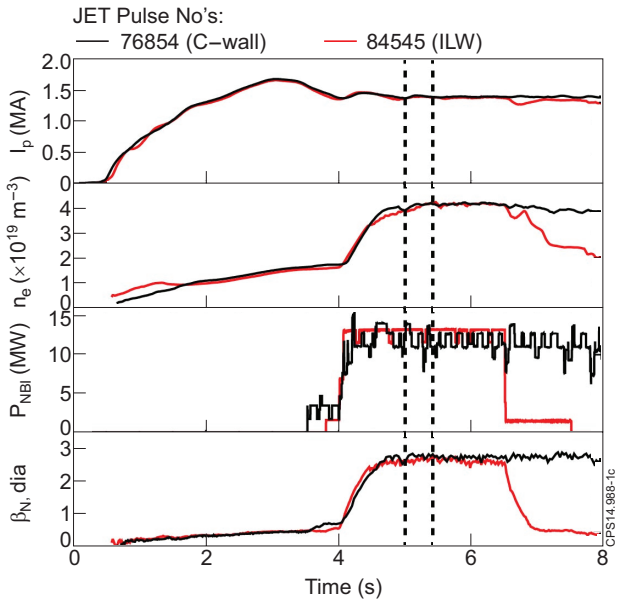

Figure 1: Time evolution of typical plasmas from the C-wall (black) and ILW (red) power scan experiments showing the plasma current, line averaged density, neutral beam heating power and β_N. The two vertical lines indicate the time window used for the confinement analysis.

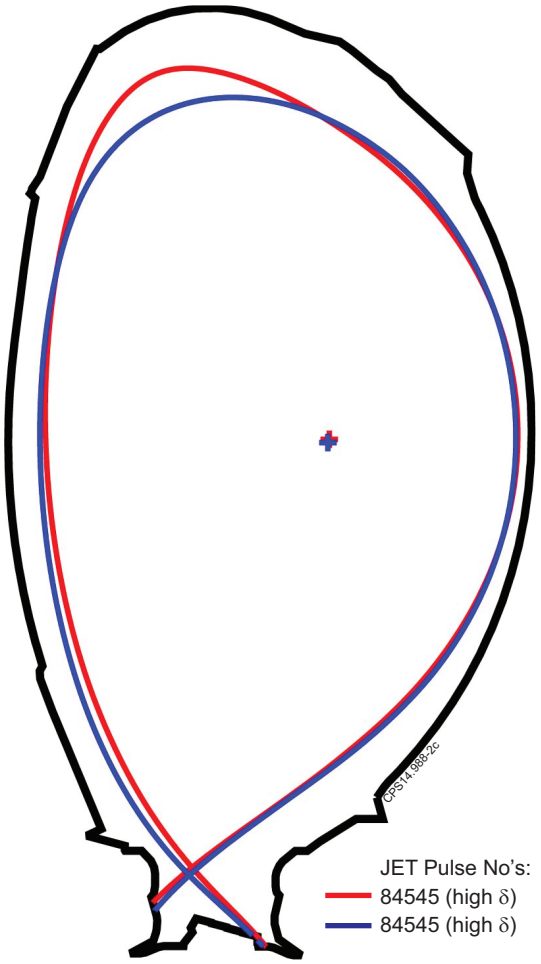

Figure 2: Typical examples of high δ (red) and low δ (blue) plasma shapes used in the power scan experiments.

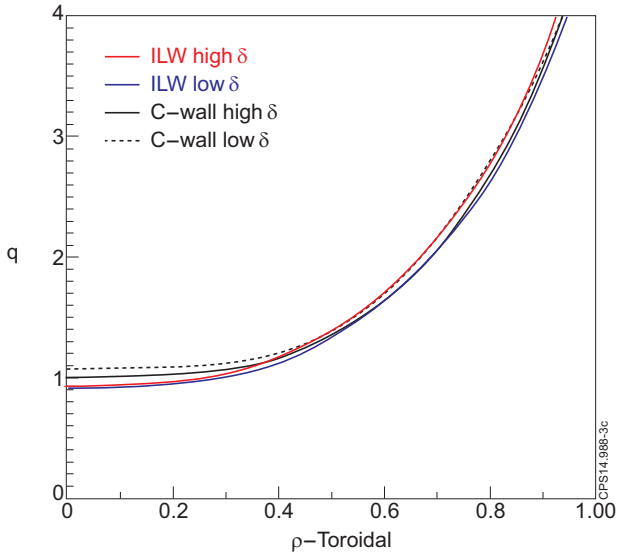

Figure 3: q-profiles at the confinement analysis time averaged over the plasmas in each of the four power scans where motional Stark effect data were available. The typical uncertainty in the determination of q_0 is estimated to be ±10%.

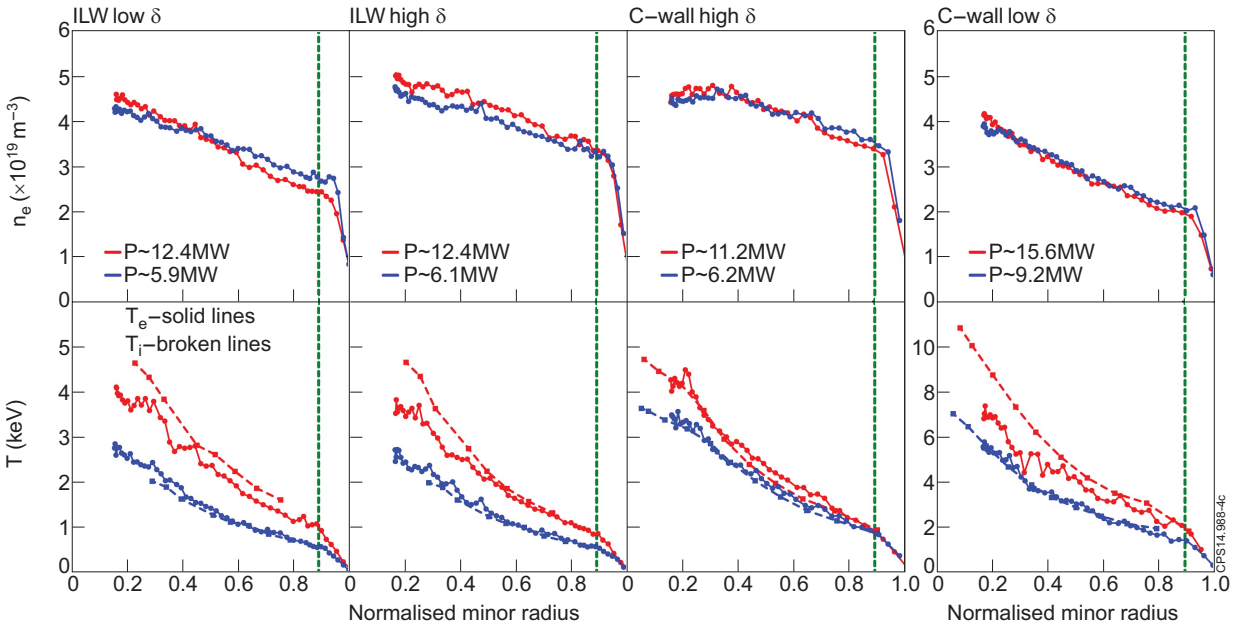

Figure 4: Density and temperature profiles at two power levels for each of the power scans. The vertical lines indicate the boundary used for the estimation of the core and pedestal energy.

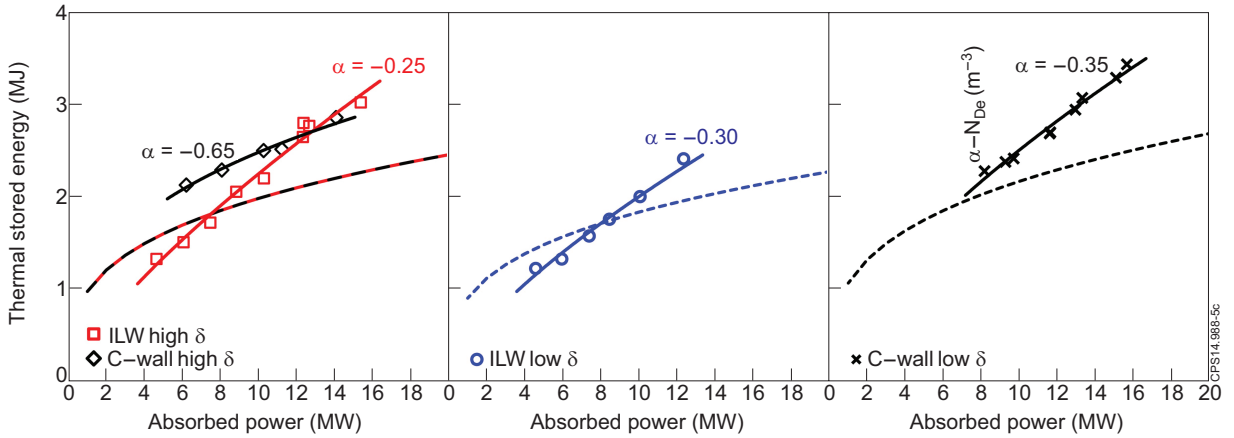

Figure 5: Plasma thermal stored energy as a function of absorbed heating power for the four power scans. The solid lines are fits to the data assuming a scaling of the form $W_{th} \sim P^{\alpha+1}$, where α is the exponent for the scaling for energy confinement time with power. The dashed lines represent the dependence using the IPB98(y,2) scaling (i.e. α = –0.69).

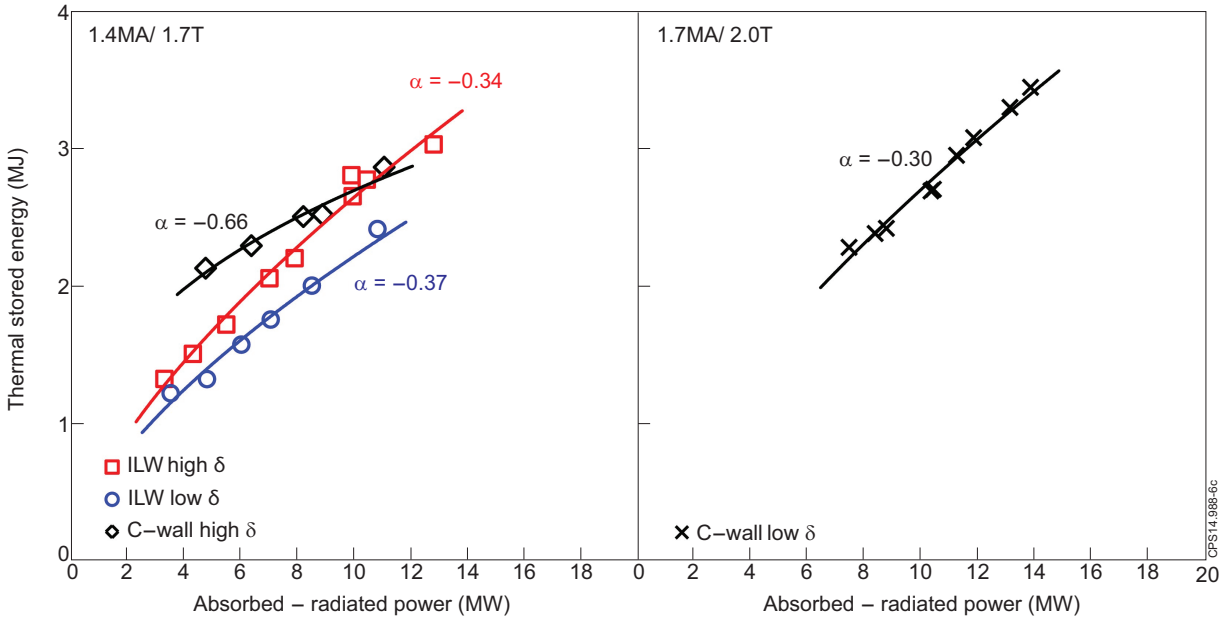

Figure 6: Plasma thermal stored energy as a function of absorbed heating power minus power radiated from within the last closed flux surface for the four power scans. The solid lines are fits to the data assuming a scaling of the form $W_{th} \sim P^{\alpha+1}$.

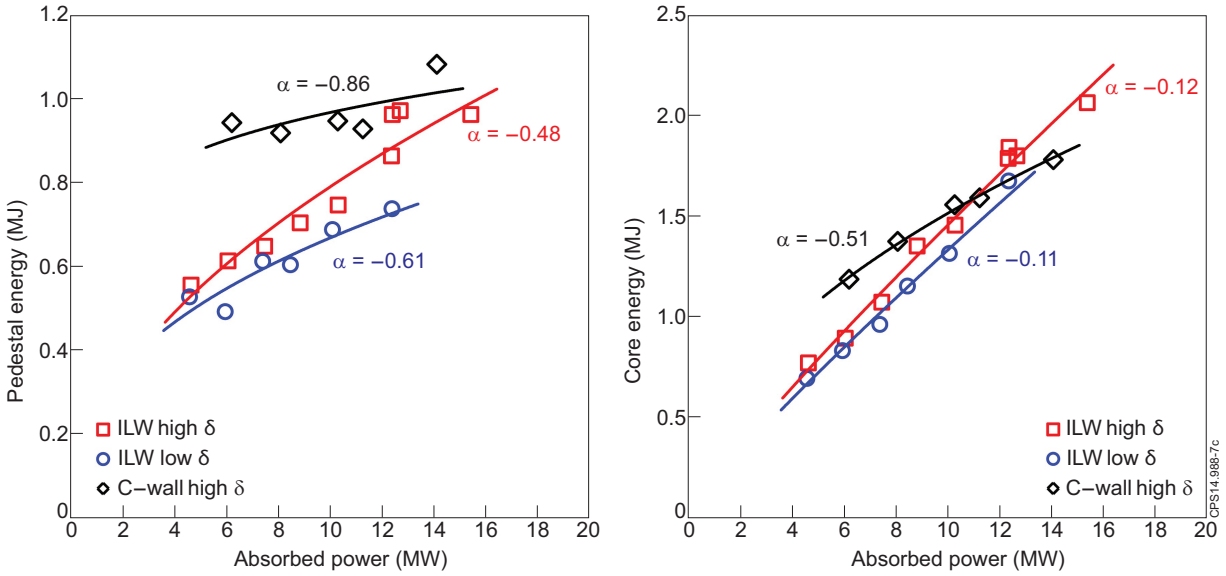

Figure 7: Pedestal energy, W_{ped}*, (left) and core energy,* W_{core}*, (right) as a function of absorbed heating power for three of the four power scans. The solid lines are fits to the data assuming a scaling of the form* $W_{ped} \sim P^{\alpha+1}$ *(left) and* $W_{core} \sim P^{\alpha+1}$ *(right).*

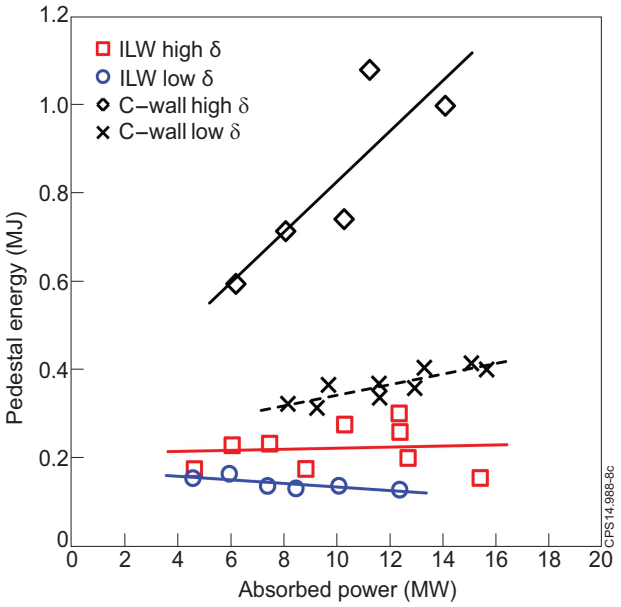

Figure 8: Dα emission from the tokamak mid-plane line-of-sight as a function of absorbed heating power the four power scans. The solid lines are linear fits to the data. Note that the magnitude of ILW Dα emission may be over-estimated due to wall reflections.

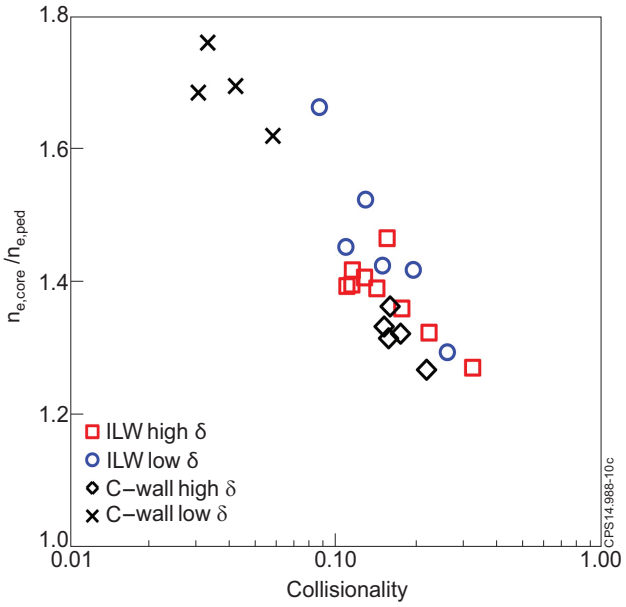

Figure 10: Electron density peaking, defined as $n_e(\rho = 0.39)/n_e(\rho = 0.89)$, as a function of plasma collisionality ($\langle \nu_{e*} \rangle = 0.012 \langle n_e \rangle Z_{eff}\, q_{95} R_0/\varepsilon^{1.5} \langle T_e \rangle^2$ where n_e is in $10^{20} m^{-3}$, T_e is in keV and R_0 is in m) for the four power scans. Pulses without high resolution Thomson scattering data are excluded for consistency.

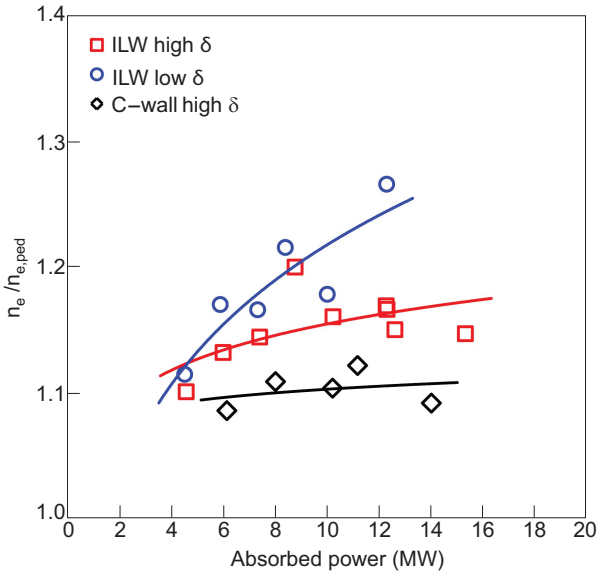

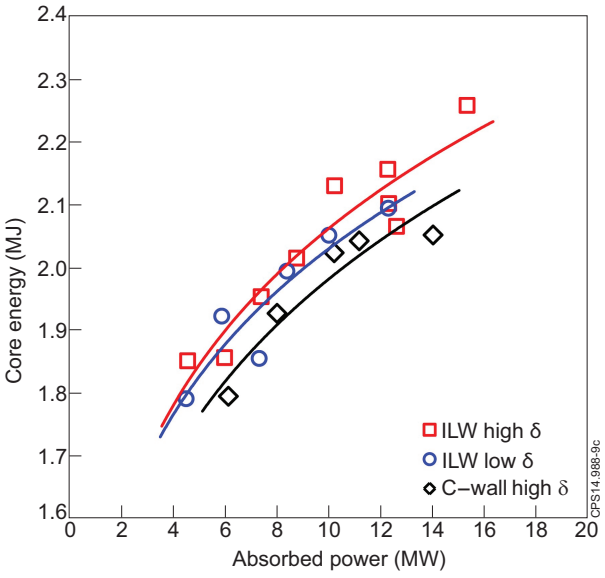

Figure 9: Electron density peaking (left), defined as $\langle n_e \rangle_V / n_e(\rho_{tor} = 0.89)$ and temperature peaking (right), defined as $\langle T_e + T_i \rangle_V / 2 \times T_e(\rho_{tor} = 0.89)$ as a function of absorbed heating power for three of the four power scans. The solid lines are fits to the data of the form $y \sim P^{\alpha}$.